Journal of Pure Applied and Industrial Physics, *Vol.11(2),1-10, February 2021* *ISSN 2229-7596 (Print)*
(An International Research Journal), *www.physics-journal.org* *ISSN 2319-7617 (Online)*

A Comparative DFT Study on the Interaction of Pristine, Al- and Ga-Doped BN Nanosheets with 5-Fluorouracil Anticancer Drug

Md. Nasir Uddin[1] and Afiya Akter Piya[1*]

[1]Department of Physics,
Mawlana Bhashani Science and Technology University,
Tangail-1902, BANGLADESH.
email: afiyaakterpiya@gmail.com.

(Received on: January 24, 2021)

ABSTRACT

Interaction of 5-fluorouracil drug (5-FU) on the pristine BN (BNNS), Al-doped BN (BN(Al)NS) and Ga-doped BN (BN(Ga)NS) nanosheets in water media was investigated. The calculated adsorption energies are about -0.48, -0.82 and -0.93 eV for 5-FU/BNNS, 5-FU/BN(Al)NS and 5-FU/BN(Ga)NS complexes respectively. The adsorption energies are greatly enhanced about 70.83% and 93.75% after doping Al and Ga atom on BN nanosheets respectively. The energy gap and work function calculations indicated that the conductivity was increased drastically after adsorption of drug molecule on the nanosheets. The energy gap decreases about 20.63%, 21.46% and 21.66% for 5-FU/BNNS, 5-FU/BN(Al)NS and 5-FU/BN(Ga)NS complexes respectively. The global indices demonstrated that the reactivity was increased during the adsorption process. Therefore, the 5-FU drug on BN(Al)NS and BN(Ga)NS can be extended as a drug delivery system.

Keywords: DFT, 5-FU, Drug delivery, BNNS, BN(Al)NS, BN(Ga)NS.

1. INTRODUCTION

An anticancer compound, 5-Fluorouracil (5-FU) has now been widely used in chemotherapy[1]. In particular, 5-FU is one of the standard pharmacological agents commonly used in cancer chemotherapy, especially in the treatment of pancreatic, stomach, breast, rectal and colorectal cancers[2–4]. It operates on cancer cells by suppressing or directly absorbing thymidylate synthase enzymes into nucleic acids[5]. Though this drug has several

side-effects, several researchers reported the great importance of 5-FU in biological fluids [6]. A nanostructure-based sensor can be used for 5-FU drug detection due to benefits such as low cost, short analysis time, quick response, miniaturization capability, high surface/volume ratio, low temperature action and high efficiency[7–10].

Recently, Boron nitride (BN) nanosheets are widely investigated in different field of sciences such as catalysts[11], dielectric materials[12], sensors[13], and hydrogen storage[14] due to their high thermal conductivity, wide band gap, excellent mechanical strength, large surface areas, high oxidation resistance and good chemical inertness[15–17]. Previous studies suggest that BN nanosheet have been used as promising candidate for drug delivery system[18–21]. Previously, Morteza Vatanparast et al. performed DFT and MD simulations to consider BN nanosheet as a drug carrier for anticancer drugs 5-fluorouracil, 6-mercaptopurine and 6-thioguanine drugs[22].

In many literature, the drug delivery application of 5-FU in chemotherapy and its mechanism and significances has been widely studied and reported[23]. Shayan and Nowroozi theoretically studied the adsorption of 5-FU on BNNTs surface. The encapsulation and adsorption of 5-FU molecule on that surface was found to be a favorable process, with a few exceptions[24]. It is also observed that doping boron nitride with Al or Ga atoms massively increase their molecular adsorption properties[25,26].

In our study, we have investigated the interaction between the 5-FU drug with the pristine BN (BNNS), Al-doped BN (BN(Al)NS) and Ga-doped BN (BN(Ga)NS). The adsorption energy with adsorption distance, charge transfer, electronic properties, global indices have been studied. The electron density map (EDM) and density of states (DOS) have been analyzed.

2. COMPUTATIONAL DETAILS

All the calculations have been performed using DFT theory as implemented in Dmol3 module[27,28]. The Perdew-Burke-Ernzerhof (PBE) functional within GGA has been considered to describe the exchange-correlation interaction[29]. We also employed the DFT semi-core pseudopotential (DSPP) for core treatment with double numerical basis set plus polarization (DNP) basis set[30]. The energy tolerance, maximum force, displacement convergence, and smearing point have been set at $2x10^{-5}$ Ha, 0.004 Ha/Å, 0.005 Å and 0.005 Ha respectively[31]. And global cut off radius of 5Å has been employed[32].

To investigate the sensitivity of the nanosheets towards the 5-FU drug, chemical potential (μ)[33] was calculated by, $\mu = -(I + A) / 2$.
Hardness (η)[34] was calculated by $\eta = (A - I)/2$.
Softness (S)[35] was calculated by $S = 1/2\eta$.
And electrophilicity (ω)[36] was calculated by following equations, $\omega = \mu^2/2\eta$

where, ionization potential, $I = E_{HOMO}$ is the energy of HOMO and electron affinity, $A = E_{LUMO}$ is the energy of LUMO.

3. RESULTS AND DISCUSSIONS

3.1 Geometric structures

Fig. 1 shows optimized structure with HOMO-LUMO and ESP map of 5-FU drug molecule. It consists of 4(C-N), 2 (N-H), 2(C-O), 2(C-C), 1(C-H) and 1 (C-F) bonds. The average bond length of C-N, N-H, C-O and C-F are 1.385, 1.02, 1.235 and 1.359 Å respectively. The HOMO level of 5-FU is located at -6.173 eV and LUMO level located at -2.491 eV. The negative charge concentrates around the O atoms while the positive charge accumulates around remaining drug which is visualized from ESP map of 5-FU.

The adsorbent nanosheets such as BNNS, BN(Al)NS and BN(Ga)NS as drug delivery carrier, are optimized in water media. Fig. 2 shows the optimized geometry with EDMs of these nanosheets. The nanosheets contain 16 hexagons. The bond distance of B-H and N-H are found as 1.202Å and 1.017Å respectively which are similar to previous studies[37]. In BN(Al)NS and BN(Ga)NS nanosheets, the Al-N and Ga-N bond distances are found to be 1.714 and 1.740Å respectively which are in good agreement with previous studies[38]. The nanosheets remain in planar after doping Al and Ga atoms on the BNNS. EDMs predict that electrons are mostly localized on the B-N bonds. Fig. 3 shows the relaxed structures of the 5-FU/BNNS, 5-FU/BN(Al)NS and 5-FU/BN(Ga)NS complexes. After adsorption of the drug on the BNNS, the nanosheet remain still planer but in case of BN(Al)NS and BN(Ga)NS, the nanosheets deform greatly and bent downward which indicates an interaction between the drug and nanosheets.

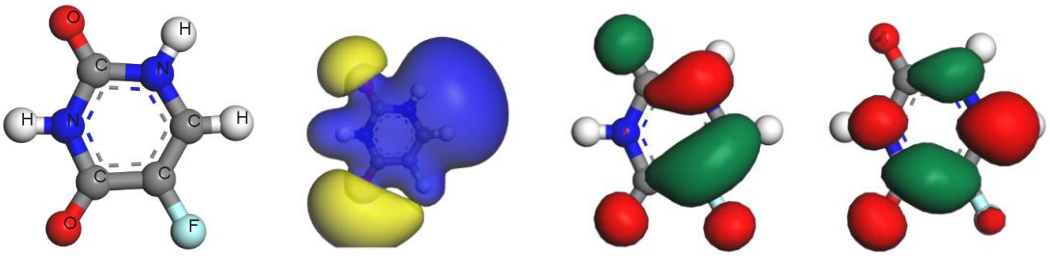

(a) (b) (c) (d)

Fig. 1. (a) Optimized structure, (b) ESP map, (c) HOMO and, (d) LUMO maps of 5-FU drug molecules.

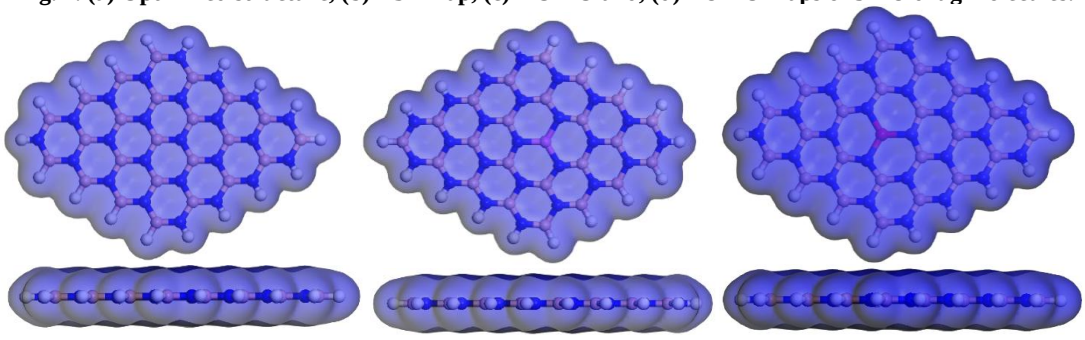

(a) (b) (c)

Fig.2. Optimized structures with EDMs of (a) BNNS, (b) BN(Al)NS and (c) BN(Ga)NS nanosheets respectively.

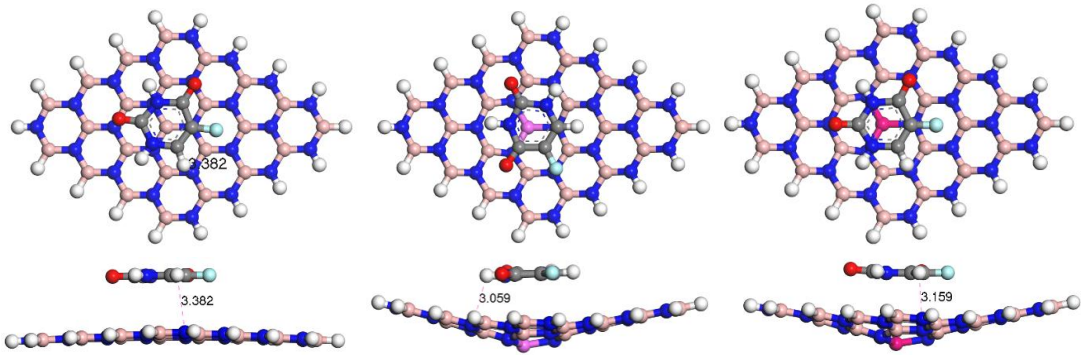

(a) (b) (c)

Fig. 3. Top (first row) and side (second row) views of (a) 5-FU/BNNS, (b) 5-FU/BN(Al)NS and (c) 5-FU/BN(Ga)NS complexes respectively.

3.2 Adsorption of 5-FU on the nanosheets

To investigate the adsorption behavior of 5-FU on the BNNS, BN(Al)NS and BN(Ga)NS nanosheets, the adsorption energy, nearest adsorption distance and charge transfer has been calculated. The adsorption energy has been calculated by using following equation[39,40],

$$E_{ad} = E_{5-FU+Nanosheet} - E_{5-FU} - E_{Nanosheet}$$

Where, E_{5-FU}, $E_{Nanosheet}$ and $E_{5-FU+Nanosheet}$ are the total energies of the 5-FU drug, nanosheets and nanosheets with the 5-FU drug molecule respectively.

The 5-FU drug molecule was placed parallel to the nanosheets and relaxed in global minima in water media. The optimized geometries were illustrated in Fig. 3. In our investigation, we found negative adsorption energies which implies an attractive and exothermic reaction between 5-FU and nanosheets. The calculated adsorption energies are -0.48, -0.82 and -0.93 eV for 5-FU/BNNS, 5-FU/BN(Al)NS and 5-FU/BN(Ga)NS respectively. The 5-FU is preferred to adsorb at a distance 3.382, 3.059 and 3.159 Å from the nanosheets. Thus, physical interaction was occurred for 5-FU/BNNS but chemisorption adsorption was occurred for 5-FU/BN(Al)NS and 5-FU/BN(Ga)NS complexes. It was clearly found that, after doping Al and Ga atoms on the BNNS, adsorption energies are drastically increased about 70.83% and 93.75% which indicates that Al and Ga dopants are largely increased the attractive interaction between the 5-FU and BN(Al)NS, and BN(Ga)NS nanosheets.

Table 1: The calculated adsorption energy (E_{ad}), minimum adsorption distance (d) and charge transfer (Δq) between 5-FU and nanosheets in water phases.

System	Water media			
	d (Å)	Δq(e)	E_{Ad} (eV)	$\%\Delta E_{Ad}$
5-FU/BNNS	3.382	-0.002	-0.48	--
5-FU/BN(Al)NS	3.059	0.007	-0.82	70.83
5-FU/BN(Ga)NS	3.159	0.004	-0.93	93.75

3.3 Charge transfer analysis

Mullekin charge analysis has been performed to investigate the net charge transfers from the 5-FU drug to the nanosheets. The amount of net charge on the 5-FU are listed in Table 1. In our calculations, 5-FU drug gains a small amount of charge about 0.002e from the BNNS. Thus 5-FU drug acts as electron acceptor and BNNS acts as electron donor. But in case of Al and Ga doped BNNS, 5-FU drug losses 0.007e and 0.004e amount of charge to the BN(Al)NS, and BN(Ga)NS nanosheets respectively. The top and side views of EDMs of the complexes are shown in Fig. 4. In EDM maps, it was clearly seen that electron hybridizations are occurred and electron density of drug and nanosheets overlaps with each other which indicates that an interaction occurs between the drug and nanosheets.

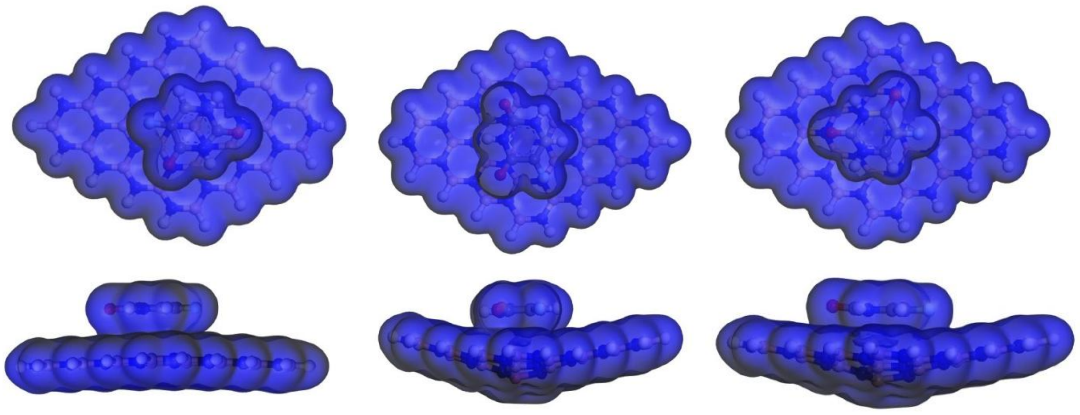

(a) (b) (c)

Fig. 4. Top (first row) and side (second row) views of EDMs of (a) 5-FU/BNNS, (b) 5-FU/ BN(Al)NS and (c) 5-FU/ BN(Ga)NS complexes respectively.

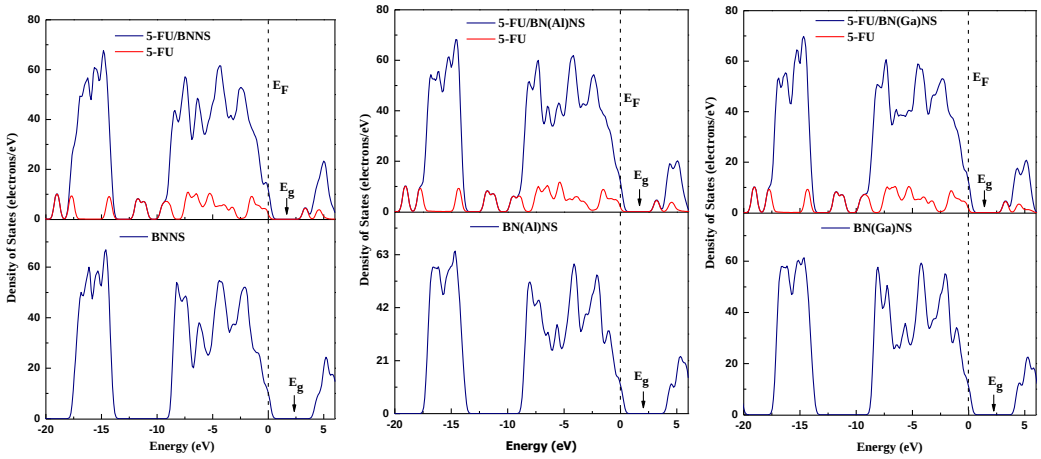

(a) (b) (c)

Fig. 5. The total and partial DOS for (a) BNNS (b) BN(Al)NS, and (c) BN(Ga)NS, nanosheets before and after adsorption of 5-FU drug molecules. The dotted line indicates the Fermi level.

3.4 Electronic Properties

The electronic properties such as HOMO energies and LUMO energies, HOMO-LUMO energy gap (E_g), work function have been analyzed. The top and side views of HOMO and LUMO of all complexes are shown in Fig. 6. In all complexes, the HOMO are localized on the nanosheets at -5.863, -5.866, -5.846 eV and LUMO are localized on drug molecules at -2.562, -2.617 and -2.605 eV for BNNS, BN(Al)NS and BN(Ga)NS respectively. The HOMO and LUMO energies are not stabilized after adsorption of 5-FU on the BNNS, BN(Al)NS and BN(Ga)NS. HOMO energies of BNNS, BN(Al)NS and BN(Ga)NS decrease slightly but the LUMO energies largely increase from -1.716, -1.743 and, -1.75 eV to -2.562, -2.617 and -2.605 eV respectively. The calculated energy gaps are 4.159, 4.137 and 4.137 eV of BNNS, BN(Al)NS and BN(Ga)NS respectively but after adsorption of 5-FU on the nanosheets, the energy gaps reduce largely about 20.63%, 21.46% and 21.66% respectively. The DOS spectra of BNNS, BN(Al)NS and BN(Ga)NS before and after adsorption of 5-FU drug are illustrated on Fig. 5. It is found that dominant peak is introduced at near to Fermi level after adsorption of 5-FU drug which is responsible for decreasing energy gap. The reduction of energy gap can exponentially enhance the conduction electron population.

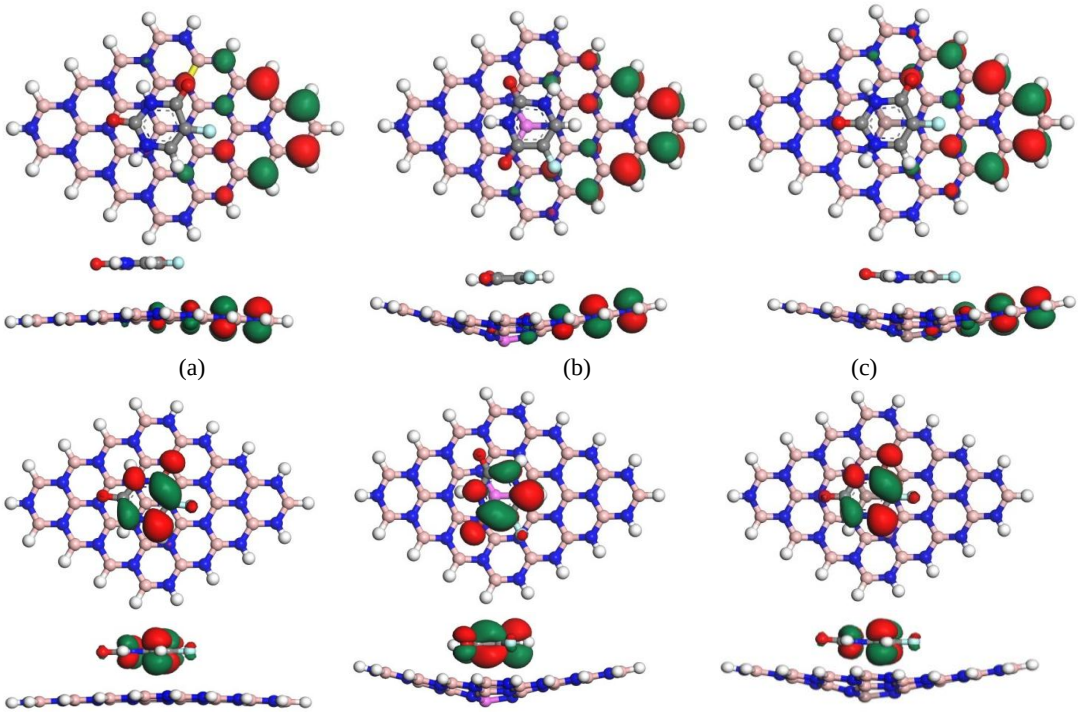

Fig. 6. Top and side views of HOMO maps (top two rows) and LUMO maps (bottom two rows) of (a, d) 5-FU/BNNS, (b, e) 5-FU/BN(Al)NS, and (c,f) 5-FU/BN(Ga)NS complexes respectively.

Table 2: HOMO energies (E_{HOMO}), LUMO energies (E_{LUMO}), HOMO-LUMO energy gap (E_g) and change in energy gap (%ΔE_g) for all complexes in water phases.

System	Water Phase						
	E_{HOMO}	E_{LUMO}	E_g	%ΔE_g	E_F (eV)	φ (eV)	% φ
5-FU	-6.173	-2.491	3.682	--	-4.331	4.331	--
BNNS	-5.875	-1.716	4.159	--	-3.792	3.792	--
BN(Al)NS	-5.88	-1.743	4.137	--	-3.813	3.813	--
BN(Ga)NS	-5.887	-1.75	4.137	--	-3.819	3.819	--
5-FU/BNNS	-5.863	-2.562	3.301	20.63	-3.798	3.798	-0.17
5-FU/BN(Al)NS	-5.866	-2.617	3.249	21.46	-4.207	4.207	-10.34
5-FU/BN(Ga)NS	-5.846	-2.605	3.241	21.66	-4.191	4.191	-9.74

3.5 Global indices

To understand the reactivity of our studied complexes, global indices such as global hardness, global softness, electrophilicity index with chemical potential and electronegativity have been analyzed and are tabulated in Table 3. Global hardness defines the resistance to deformation of electron cloud of system in presence of external perturbation[41]. High value of global hardness means that the chemical stability of the structure increases with decreasing the reactivity[42]. There is an opposite relationship of hardness with global softness and electrophilicity index. Higher value of the softness and electrophilicity indicates the higher reactivity of the complexes. The calculated values of global indices and chemical potential are almost same for the three nanosheets, BNNS, BN(Al)NS and BN(Ga)NS. But during the adsorption of the drug molecule on the nanosheets, the hardness decreases and softness increases which means, the chemical reactivity increases during the adsorption process. The calculated hardness are 5.017, 5.009 and 5.012 eV for BNNS, BN(Al)NS and BN(Ga)NS respectively. But during adsorption process, the hardness decreases to 4.582, 4.558 and 4.544 eV respectively. On the other hand the softness of the nanosheets during adsorption of drug increases from 0.099 to 0.1091, 0.099 to 0.1097, 0.099 to 0.1100 eV^{-1} for BNNS, BN(Al)NS and BN(Ga)NS respectively. Thus, dopants Al and Ga atoms are enhanced the reactivity of BNNS towards the 5-FU drug.

Table 3: Computed chemical potential (μ), electronegativity (χ), global hardness (η), global softness (S), electrophilicity index (ω) of the studied complexes.

System	Water media				
	μ (eV)	χ (eV)	η (eV)	ω (eV)	S (eV^{-1})
5-FU	-4.332	4.332	4.9275	46.235	0.1015
BNNS	-3.7955	3.7955	5.017	36.137	0.0996
BN(Al)NS	-3.8115	3.8115	5.0085	36.381	0.0998
BN(Ga)NS	-3.8185	3.8185	5.012	36.539	0.0998
5-FU/BNNS	-4.2125	4.2125	4.582	40.654	0.1091
5-FU/BN(Al)NS	-4.2415	4.2415	4.5575	40.995	0.1097
5-FU/BN(Ga)NS	-4.2255	4.2255	4.5435	40.562	0.1100

4 CONCLUSIONS

Interaction of 5-FU on the BNNS, BN(Al)NS and BN(Ga)NS in water media was investigated. The calculated adsorption energies are found about -0.48, -0.82 and -0.93 eV for 5-FU/BNNS,5-FU/BN(Al)NS and 5-FU/BN(Ga)NS complexes respectively. The adsorption energies are greatly enhanced about 70.83% and 93.75% after doping Al and Ga atom on BN nanosheets respectively. The energy gap and work function calculations indicated that the conductivity was increased drastically after adsorption of drug molecule on the nanosheets. The energy gap decreases about 20.63%, 21.46% and 21.66% for 5-FU/BNNS,5-FU/BN(Al)NS and 5-FU/BN(Ga)NS complexes respectively. The global indices demonstrated that the reactivity was increased during the adsorption process. Therefore, the 5-FU drug on BN(Al)NS and BN(Ga)NS can be extended as a drug delivery system.

REFERENCES

1. V. Selvaraj and M. Alagar, "Analytical detection and biological assay of antileukemic drug 5-fluorouracil using gold nanoparticles as probe," *Int. J. Pharm.*, vol. 337, no. 1–2, pp. 275–281, (2007).
2. C. Heidelberger and F. J. Ansfield, "Experimental and Clinical Use of Fluorinated Pyrimidines in Cancer Chemotherapy.," *Cancer Res.*, vol. 23, pp. 1226–1243, (1963).
3. V. P. Pattar and S. T. Nandibewoor, "Electroanalytical method for the determination of 5-fluorouracil using a reduced graphene oxide/chitosan modified sensor," *RSC Adv.*, vol. 5, no. 43, pp. 34292–34301, (2015).
4. X. Hua, X. Hou, X. Gong, and G. Shen, "Electrochemical behavior of 5-fluorouracil on a glassy carbon electrode modified with bromothymol blue and multi-walled carbon nanotubes," *Anal. Methods*, vol. 5, no. 10, pp. 2470–2476, (2013).
5. D. B. Longley, D. P. Harkin, and P. G. Johnston, "5-Fluorouracil: Mechanisms of action and clinical strategies," *Nature Reviews Cancer*, vol. 3, no. 5. pp. 330–338, (2003).
6. B. B. Prasad, D. Kumar, R. Madhuri, and M. P. Tiwari, "Nonhydrolytic sol-gel derived imprinted polymer-multiwalled carbon nanotubes composite fiber sensors for electrochemical sensing of uracil and 5-fluorouracil," *Electrochim. Acta*, vol. 71, pp. 106–115, (2012).
7. R. Rostamoghli, M. Vakili, A. Banaei, E. Pourbashir, and K. Jalalierad, "Applying the B12N12 nanoparticle as the CO, CO2, H2O and NH3 sensor," *Chem Rev Lett*, vol. 1, pp. 31–36, (2018).
8. J. Beheshtian, A. A. Peyghan, and Z. Bagheri, "Arsenic interactions with a fullerene-like BN cage in the vacuum and aqueous phase," *J. Mol. Model.*, vol. 19, no. 2, pp. 833–837, (2013).
9. J. Beheshtian, M. T. Baei, A. A. Peyghan, and Z. Bagheri, "Nitrous oxide adsorption on pristine and Si-doped AlN nanotubes," *J. Mol.Model.*, vol. 19, no.2, pp. 943-949, (2013).
10. M. Noei and A. A. Peyghan, "A DFT study on the sensing behavior of a BC2N nanotube toward formaldehyde," *J. Mol. Model.*, vol. 19, no. 9, pp. 3843–3850, (2013).

11. P. Marbaniang *et al.*, "Nanorice-like Structure of Carbon-Doped Hexagonal Boron Nitride as an Efficient Metal-Free Catalyst for Oxygen Electroreduction," *ACS Sustain. Chem. Eng.*, vol. 6, no. 8, pp. 11115–11122, (2018).
12. F. Hui, C. Pan, Y. Shi, Y. Ji, E. Grustan-Gutierrez, and M. Lanza, "On the use of two dimensional hexagonal boron nitride as dielectric," *Microelectronic Engineering*, vol. 163. pp. 119–133, (2016).
13. Y. Zhang *et al.*, "Copper/hexagonal boron nitride nanosheet composite as an electrochemical sensor for nitrite determination," *Int. J. Electrochem. Sci.*, vol. 13, no. 6, pp. 5995–6004, (2018).
14. P. Ahmad *et al.*, "Synthesis of multilayered hexagonal boron nitride microcrystals as a potential hydrogen storage element," *Ceram. Int.*, vol. 43, no. 9, pp. 7358–7361, (2017).
15. C. R. Dean *et al.*, "Boron nitride substrates for high-quality graphene electronics," *Nat. Nanotechnol.*, vol. 5, no. 10, pp. 722–726, (2010).
16. A. Pakdel, C. Zhi, Y. Bando, T. Nakayama, and D. Golberg, "Boron nitride nanosheet coatings with controllable water repellency," *ACS Nano*, vol. 5, no. 8, pp. 6507–6515, (2011).
17. J. Yu *et al.*, "Vertically aligned boron nitride nanosheets: Chemical vapor synthesis, ultraviolet light emission, and superhydrophobicity," *ACS Nano*, vol. 4, no. 1, pp. 414–422, (2010).
18. E. S. Permyakova *et al.*, "Synthesis and Characterization of Folate Conjugated Boron Nitride Nanocarriers for Targeted Drug Delivery," *J. Phys. Chem. C*, vol. 121, no. 50, pp. 28096–28105, (2017).
19. Q. Weng *et al.*, "Highly water-soluble, porous, and biocompatible boron nitrides for anticancer drug delivery," *ACS Nano*, vol. 8, no. 6, pp. 6123–6130, (2014).
20. M. Jedrzejczak-Silicka, M. Trukawka, M. Dudziak, K. Piotrowska, and E. Mijowska, "Hexagonal boron nitride functionalized with Au nanoparticles—properties and potential biological applications," *Nanomaterials*, vol. 8, no. 8, (2018).
21. T. T. Tran, K. Bray, M. J. Ford, M. Toth, and I. Aharonovich, "Quantum emission from hexagonal boron nitride monolayers," *Nat. Nanotechnol.*, vol. 11, no. 1, pp.37-41, (2016).
22. M. Vatanparast and Z. Shariatinia, "Hexagonal boron nitride nanosheet as novel drug delivery system for anticancer drugs: Insights from DFT calculations and molecular dynamics simulations," *J. Mol. Graph. Model.*, vol. 89, pp. 50–59, (2019).
23. B. Hatamluyi, Z. Es'haghi, F. Modarres Zahed, and M. Darroudi, "A novel electrochemical sensor based on GQDs-PANI/ZnO-NCs modified glassy carbon electrode for simultaneous determination of Irinotecan and 5-Fluorouracil in biological samples," *Sensors Actuators, B Chem.*, vol. 286, pp. 540–549, (2019).
24. K. Shayan and A. Nowroozi, "Boron nitride nanotubes for delivery of 5-fluorouracil as anticancer drug: a theoretical study," *Appl. Surf. Sci.*, vol. 428, pp. 500–513, (2018).
25. A. A. Darwish, M. M. Fadlallah, A. Badawi, and A. A. Maarouf, "Adsorption of sugars on Al- and Ga-doped boron nitride surfaces: A computational study," *Appl. Surf. Sci.*, vol. 377, pp. 9–16, (2016).
26. F. Behmagham, E. Vessally, B. Massoumi, A. Hosseinian, and L. Edjlali, "A computational study on the SO2 adsorption by the pristine, Al, and Si doped BN

nanosheets," *Superlattices Microstruct.*, vol. 100, pp. 350–357, (2016).
27. B. Delley, "An all-electron numerical method for solving the local density functional for polyatomic molecules," *J. Chem. Phys.*, vol. 92, no. 1, pp. 508–517, (1990).
28. B. Delley, "From molecules to solids with the DMol3 approach," *J. Chem. Phys.*, vol. 113, no. 18, pp. 7756–7764, (2000).
29. J. P. Perdew, K. Burke, and M. Ernzerhof, "Generalized gradient approximation made simple," *Phys. Rev. Lett.*, vol. 77, no. 18, pp. 3865–3868, (1996).
30. B. Delley, "Hardness conserving semilocal pseudopotentials," *Phys. Rev. B - Condens. Matter Mater. Phys.*, vol. 66, no. 15, pp. 1–9, (2002).
31. Q. Zhou, W. Ju, X. Su, Y. Yong, and X. Li, "Adsorption behavior of SO2 on vacancy-defected graphene: A DFT study," *J. Phys. Chem. Solids*, vol. 109, pp. 40–45, (2017).
32. X. Chen *et al.*, "The electronic and optical properties of silicene/g-ZnS heterobilayers: A theoretical study," *J. Mater. Chem. C*, vol. 4, no. 29, pp. 7004–7012, (2016).
33. R. G. Pearson, "Absolute Electronegativity and Hardness: Application to Inorganic Chemistry," *Inorg. Chem.*, vol. 27, no. 4, pp. 734–740, (1988).
34. P. K. Chattaraj and R. G. Parr, "Density functional theory of chemical hardness," in *Chemical Hardness*, pp. 11–25 (2006).
35. W. R. Wadt and P. J. Hay, "Ab initio effective core potentials for molecular calculations. Potentials for main group elements Na to Bi," *J. Chem. Phys.*, vol. 82, no. 1, pp. 284–298, (1985).
36. A. S. Rad, S. S. Shabestari, S. A. Jafari, M. R. Zardoost, and A. Mirabi, "N-doped graphene as a nanostructure adsorbent for carbon monoxide: DFT calculations," *Mol. Phys.*, vol. 114, no. 11, pp. 1756–1762, (2016).
37. M. R. Hossain *et al.*, "Adsorption behaviour of metronidazole drug molecule on the surface of hydrogenated graphene, boron nitride and boron carbide nanosheets in gaseous and aqueous medium: A comparative DFT and QTAIM insight," *Phys. E Low-Dimensional Syst. Nanostructures*, vol. 126, (2021).
38. E. Nemati-Kande, M. Abbasi, and M. D. Mohammadi, "DFT studies on the interactions of pristine, Al and Ga-doped boron nitride nanosheets with CH3X (X=F, Cl and Br)," *J. Mol. Struct.*, vol. 1199, (2020).
39. S. U. D. Shamim *et al.*, "A DFT study on the geometrical structures, electronic, and spectroscopic properties of inverse sandwich monocyclic boron nanoclusters ConBm (n = 1.2; m = 6–8)," *J. Mol. Model.*, vol. 26, no. 6, (2020).
40. S. U. Daula Shamim, M. K. Hossain, S. M. Hasan, A. Hossain, and F. Ahmed, "Ab initio study of N-doped graphene oxide (NDGO) as a promising anode material for Li-ion rechargeable battery," *Mol. Simul.*, vol. 46, no. 14, pp. 1135–1145, (2020).
41. N. Islam and D. C. Ghosh, "The Electronegativity and the Global Hardness Are Periodic Properties of Atoms," *J. Quantum Inf. Sci.*, vol. 1, no. 3, pp. 135–141, (2011).
42. A. Shokuhi Rad, S. Alijantabar Aghouzi, N. Motaghedi, S. Maleki, and M. Peyravi, "Theoretical study of chemisorption of cyanuric fluoride and S-triazine on the surface of Al-doped graphene," *Mol. Simul.*, vol. 42, no. 18, pp. 1519–1527, (2016).